SIAM J. APPL. MATH.
Vol. 62, No. 6, pp. 1872–1898

EXPONENTIAL ASYMPTOTICS AND CAPILLARY WAVES*

S. J. CHAPMAN† AND J.-M. VANDEN-BROECK‡

Abstract. Recently developed techniques in exponential asymptotics beyond all orders are employed on the problem of potential flows with a free surface and small surface tension, in the absence of gravity. Exponentially small capillary waves are found to be generated on the free surface where the equipotentials from singularities in the flow (for example, stagnation points and corners) meet it. The amplitude of these waves is determined, and the implications are considered for many quite general flows. The asymptotic results are compared to numerical simulations of the full problem for flow over a polygonal plough and for flow round a right-angled corner, and they show remarkably good agreement, even for quite large values of the surface tension parameter.

Key words. exponentially small, Stokes lines, optimal truncation, divergent expansions, singular perturbation, surface tension

AMS subject classifications. 76B07, 76B45, 41A60, 35B25

PII. S003613990038116X

1. Introduction.

We consider the problem of potential flows with a free surface, in the absence of gravity, but with small surface tension. Examples of such flows (which we will consider in section 6) include ploughing flows, flow over a submerged body, flow around a corner, gliding or planing flows, and impinging jets. However, for much of the paper the precise geometry of the flow is unimportant and may be left unspecified.

We will be concerned with the limit in which the surface tension parameter tends to zero. In this limit the problem is a singular perturbation problem, and therefore we would expect the formal asymptotic series developed in powers of the surface tension parameter to be divergent. This divergence is associated with the presence of an exponentially small correction to the algebraic expansion, which appears "beyond all orders" [9].

Kruskal and Segur [14] observed that in nonlinear ordinary differential equations the divergence is associated with a singularity in the analytic continuation of the leading-order solution, near which the formal asymptotic series breaks down. They formulate an inner problem in the vicinity of the singularity and find that its solution contains a decaying exponential in the far field, in addition to the terms which match with the algebraic series. This exponential is matched to a solution of the linearized equation away from the singularity to obtain the exponentially small, beyond all orders correction. Kruskal and Segur solve the inner problem numerically (observing the exponential along a ray on which the algebraic terms vanished), but other authors have since observed that the far field of the inner solution can be Borel-summed to obtain the exponential to be matched to the outer solution (see, for example, [8, 11]).

A similar method is formulated in [5, 4], where the algebraic asymptotic expansion (away from the singularity) is optimally truncated (that is, truncated at its least term), which results in an exponentially small error between the truncated series and

*Received by the editors November 10, 2000; accepted for publication (in revised form) January 24, 2002; published electronically July 3, 2002.
http://www.siam.org/journals/siap/62-6/38116.html
†Mathematical Institute, Center for Industrial and Applied Mathematics, Oxford University, 24-29 St. Giles', Oxford OX1 3LB, United Kingdom (chapman@maths.ox.ac.uk).
‡School of Mathematics, University of East Anglia, Norwich, England NR4 7TJ, United Kingdom (J.Vanden-broeck@uea.ac.uk).

the exact solution. This allows the exponentially small corrections to be observed switching on across Stokes lines by smoothing the Stokes discontinuity, and is a generalization of the smoothing of Stokes discontinuities in linear ordinary differential equations discovered by Berry [2]. We also note that a general framework for determining exponentially small terms in rank-1 ordinary differential equations has been recently given by Costin [6].

The exponentially small correction terms which appear in the present problem correspond to capillary waves on the free surface of exponentially small amplitude. We will find that we are able to determine quite simply the region of the free surface they occupy, as well as their magnitude, even for very general flow geometries. We note that exponentially small gravity-capillary waves have been studied in the context of the Korteweg–de Vries equation in [1, 3, 10, 17].

The rest of the paper is organized as follows. In section 2 we formulate the problem mathematically. In section 3 and section 4 we apply the procedure developed in [5]. In section 3 we naively expand the solution as a formal power series in the surface tension parameter and find the form of the late terms in this series. This enables us, in section 4, to truncate the algebraic series optimally and to observe the subdominant exponentials being switched on across Stokes lines. In section 5 we compare the results of section 4 with a direct numerical simulation of the full problem for two particular flows, namely, flow over a polygonal plough and flow round a right-angled corner. We will find that there is remarkable agreement between the asymptotic and numerical results, even for quite large values of the surface tension parameter. The flow past a polygonal plough was considered before by Tuck and Vanden-Broeck [16] in the absence of surface tension but with the effect of gravity included.

In section 6 we consider the implications of the results of section 4 for many other examples of potential flows with a free surface. Finally, in section 7, we present out conclusions.

2. Formulation of the problem. In the fluid region, we have steady, incompressible, irrotational, inviscid flow, so that the fluid velocity $\boldsymbol{u} = (u, v) = \nabla\phi$, where the velocity potential ϕ satisfies

$$\nabla^2\phi = 0.$$

On all boundaries we have the kinematic condition

$$\frac{\partial\phi}{\partial n} = 0, \tag{2.1}$$

while on the free boundary we also have the dynamic condition, which from Bernoulli's equation is

$$\frac{1}{2}|\nabla\phi|^2 - \frac{1}{2} = -\epsilon\kappa, \tag{2.2}$$

where the skin speed of the unperturbed free boundary has been normalized to unity, ϵ is the surface tension parameter, and κ is the curvature, positive if the center of curvature lies in the fluid region. As usual we define the complex potential by $w = \phi + i\psi$, where ψ is the streamfunction (with ψ chosen to be zero on the free boundary), and we let $z = x + iy$. Since w is then an analytic function of z the map $z \to w$ is a conformal transformation of the flow region to a region of the potential plane. A second transformation $w \to \zeta$ is often used to map this region to the upper half ζ-plane.

It is convenient to work in terms of the complex velocity $dw/dz = u - iv$, which may be written as $qe^{-i\theta}$, where θ is the angle the streamlines make with the x-axis. The analyticity of $qe^{-i\theta}$ in the upper half ζ-plane implies

$$\log q = -\frac{1}{\pi}\int_{-\infty}^{\infty} \frac{\theta(\xi')\,d\xi'}{\xi' - \xi}, \tag{2.3}$$

where $\zeta = \xi + i\eta$, while (2.1) implies that on the free boundary θ is the angle the tangent makes with the x-axis (i.e., the free boundary is a streamline). Then (2.2) is

$$q^2 - 1 = -2\epsilon\frac{d\theta}{ds} \tag{2.4}$$

on the free boundary, where s is arclength, increasing in the flow direction, and we have assumed that the fluid region lies to the left of the free boundary as s increases. Note that this implies that in the flow region $\psi > 0$, i.e., that the upper half ζ-plane corresponds to a region in the upper half w-plane. Noting that

$$\frac{d\theta}{ds} = \frac{d\theta}{d\phi}\frac{\partial\phi}{\partial s} = q\frac{d\theta}{d\phi}$$

in the potential plane (with q positive on the free boundary), this is

$$q^2 - 1 = -2\epsilon q\frac{d\theta}{d\phi}. \tag{2.5}$$

We will see in the next section that Stokes lines originate at singularities in the analytic continuation of θ and q satisfying (2.3) and (2.5), that is, on the analytic continuation of the free boundary. Thus we will consider (2.3) and (2.5) for complex ξ and ϕ and complex q and θ. Since we are dealing with analytic complex variables z, ζ, and w anyway, this can lead to some confusion, but this also means that the analytic continuation is much simpler than in problems with other field equations. Since ϕ is already the real part of the analytic variable w, ξ the real part of the analytic variable ζ, the complexified ϕ can be identified with w and the complexified ξ can be identified with ζ. The difference between the complexified free boundary and the flow region is that on the complexified free boundary q and θ are not real, even though $qe^{-i\theta}$ is still equal to dw/dz.

Analytically continuing (2.3) into the upper half ξ-plane gives

$$\log q - i\theta = -\frac{1}{\pi}\int_{-\infty}^{\infty} \frac{\theta(\zeta')\,d\zeta'}{\zeta' - \zeta}, \tag{2.6}$$

where we have replaced ξ by ζ to emphasize that it is now complex. Similarly, we will write (2.5) for complex ϕ by replacing ϕ by w so that

$$q^2 - 1 = -2\epsilon q\frac{d\theta}{dw}. \tag{2.7}$$

Note that the right-hand side of (2.6) may alternatively be written

$$-\frac{1}{\pi}\int_{-\infty}^{\infty} \frac{\theta(\zeta')\,d\zeta'}{\zeta' - \zeta} = -\frac{i}{\pi}\int_{-\infty}^{\infty} \frac{\log q(\zeta')\,d\zeta'}{\zeta' - \zeta} = \frac{1}{2\pi i}\int_{-\infty}^{\infty} \frac{\log q(\zeta') - i\theta(\zeta')}{\zeta' - \zeta}\,d\zeta',$$

since

$$\int_{-\infty}^{\infty} \frac{\log q(\zeta') + i\theta(\zeta')}{\zeta' - \zeta}\, d\zeta' = 0$$

because

$$\frac{\log q(\zeta') - i\theta(\zeta')}{\zeta' - \bar{\zeta}}$$

is analytic in the upper half plane. However, we will use the form (2.6) for the remainder of the paper.

Finally we note that in some of our examples the fluid lies on the right of the free boundary for increasing s. In this case (2.7) becomes

$$q^2 - 1 = 2\epsilon q \frac{d\theta}{dw} \tag{2.8}$$

and $\psi < 0$ in the flow; i.e., the upper half ζ-plane corresponds to a region in the lower half w-plane. This corresponds simply to letting $w \to -w$, so that the results we obtain are easily translated to this case.

3. Asymptotic expansion for small surface tension. We will solve (2.6), (2.7) asymptotically as $\epsilon \to 0$. The first step in applying the procedure developed in [5] is to determine the algebraic expansion in powers of ϵ, and in particular the form of the late terms in this expansion, so that we can truncate it optimally.

3.1. Late terms in the regular asymptotic expansion. The first step is to naively expand in powers of ϵ as

$$\theta = \sum_{n=0}^{\infty} \epsilon^n \theta_n, \qquad q = \sum_{n=0}^{\infty} \epsilon^n q_n. \tag{3.1}$$

Then

$$q_0 = 1, \tag{3.2}$$

$$0 = -\frac{1}{\pi} \fint_{-\infty}^{\infty} \frac{\theta_0(\xi')\, d\xi'}{\xi' - \xi}, \tag{3.3}$$

$$q_1 = -\frac{d\theta_0}{dw}, \tag{3.4}$$

$$\frac{q_1}{q_0} - i\theta_1 = -\frac{1}{\pi} \int_{-\infty}^{\infty} \frac{\theta_1(\zeta')\, d\zeta'}{\zeta' - \zeta}, \tag{3.5}$$

$$q_0 q_2 + \frac{q_1^2}{2} = -q_0 \frac{d\theta_1}{dw} - q_1 \frac{d\theta_0}{dw}, \tag{3.6}$$

$$q_0 q_n + q_1 q_{n-1} + \cdots = -q_0 \frac{d\theta_{n-1}}{dw} - q_1 \frac{d\theta_{n-2}}{dw} - \cdots - q_{n-1} \frac{d\theta_0}{dw}, \quad n \geq 3. \tag{3.7}$$

$$\frac{q_n}{q_0} - \frac{q_{n-1} q_1}{q_0^2} + \cdots - i\theta_n = -\frac{1}{\pi} \int_{-\infty}^{\infty} \frac{\theta_n(\zeta')\, d\zeta'}{\zeta' - \zeta}, \quad n \geq 2. \tag{3.8}$$

Note that the solution of (3.3) is not just $\theta_0 = 0$. In mapping the fluid region to the upper half plane the free surface will be mapped to a section of the real axis but not

to the whole real axis. Fixed boundaries will also be mapped to the real axis, and on these boundaries θ_0 is known and has logarithmic singularities. (The existence of logarithmic singularities allows the existence of a nonzero solution to (3.3) while not invalidating (2.3).) Thus when the geometry is specified (3.3) will state that an integral of θ_0 over part of the real line is equal to a known right-hand side. See, for example, (5.6).

In order to truncate the series (3.1) optimally we need to know the behavior of the late terms in the expansion; i.e., we need to solve (3.7) and (3.8) as $n \to \infty$. The omitted terms in (3.7), (3.8) can readily be calculated (they arise from expanding the log in (2.6) and the products in (2.7)), but we will see that they are all of lower order in n for large n.

Now, in the leading-order problem θ_0 may have singularities as a function of w (through the conformal map ζ). However, all higher-order problems are linear and can therefore introduce no new singularities in θ. Thus the singular points of $\theta_n(w)$ must be the same as those of $\theta_0(w)$ for all n. The singular perturbation in (2.7) means that to determine each successive term in the expansion we differentiate the previous term. Thus, if θ_n has a singularity of the form $1/(w-w_0)^n$, then θ_{n+1} will have a singularity of the form $n/(w-w_0)^{n+1}$. Thus as $n \to \infty$ we expect the asymptotic expansions (3.1) to exhibit factorial/power divergence, so that we make the ansatz

$$\theta_n \sim \frac{\Theta\Gamma(n+\gamma)}{\chi^{n+\gamma}}, \qquad q_n \sim \frac{Q\Gamma(n+\gamma)}{\chi^{n+\gamma}} \quad \text{as } n \to \infty, \tag{3.9}$$

where χ, γ, Θ, and Q are functions of w but are independent of n. We will find that the terms on the left-hand side of (3.8) exponentially dominate those on the right-hand side as $n \to \infty$, so that

$$q_n \sim i\theta_n + q_{n-1}q_1 + \cdots \qquad \text{as } n \to \infty. \tag{3.10}$$

Then at leading order in (3.7) using (3.10) and the ansatz (3.9) we have

$$\frac{d\chi}{dw} = i,$$

so that

$$\chi = iw + \text{constant}.$$

Since the singularities of θ_n are the same as those of θ_0 we know that χ must vanish at one of these singularities. In general the late terms will be a sum of terms such as (3.9), one centered on each singularity of θ_0. On the free boundary (i.e., for real w) this sum is dominated by those singularities closest to the real axis (i.e., with the smallest value of ψ). Denote by w_0 the closest singularity to the real axis in the upper half w-plane (since we are in the upper half ζ-plane). Then

$$\chi = i(w - w_0). \tag{3.11}$$

At order $\log n/n$ in (3.7) we find $d\gamma/dw = 0$, so that γ is in fact a constant. At order $1/n$ we find

$$i\Theta q_1 + i\Theta q_1 = -\frac{d\Theta}{dw} + q_1\Theta\chi' - i\Theta\frac{d\theta_0}{dw},$$

i.e.,

$$\frac{d\Theta}{dw} = -i\Theta\left(q_1 + \frac{d\theta_0}{dw}\right) = 0,$$

by (3.4). Hence $\Theta = \text{constant} = \Lambda$, say.

In summary we have

$$\theta_n \sim \frac{\Lambda\Gamma(n+\gamma)}{(i(w-w_0))^{n+\gamma}}, \qquad q_n \sim \frac{i\Lambda\Gamma(n+\gamma)}{(i(w-w_0))^{n+\gamma}} \quad \text{as } n \to \infty. \tag{3.12}$$

To determine γ we need to examine the order of the singularity in θ_0 as $w \to w_0$, which we will do in section 3.2. To determine Λ we must match with an inner region in the vicinity of w_0, which we will do in section 3.3.

3.2. Inner limit of θ_0. To determine γ we need to examine the order of the singularity in θ_0 as $w \to w_0$. This will depend on the type of singularity in the flow field. Typical singularities include stagnation points, sources, sinks, and flow around the corner of an obstacle.

For stagnation points and flow around corners, locally in the vicinity of the singularity we have $w - w_0 = \text{const.} \times (z - z_0)^k$ for some $k \neq 1$. For a stagnation point generically $k = 2$, while for flow around a corner $k = \pi/\beta$, where β is the interior (i.e., in the fluid) angle of the corner. Then, for the corresponding singularity on the analytic continuation of the free boundary

$$\frac{dw}{dz} = q_0 e^{-i\theta_0} = e^{-i\theta_0} = \text{const.} \times (z - z_0)^{k-1} = \text{const.} \times (w - w_0)^{(k-1)/k},$$

remembering that $q_0 = 1$ on the free boundary. Hence

$$\theta_0 \sim i\frac{(k-1)}{k}\log(w - w_0), \tag{3.13}$$

as $w \to w_0$. For (3.13) to be compatible with (3.12) we must have $\gamma = 0$, giving

$$\theta_n \sim \frac{\Lambda\Gamma(n)}{(i(w-w_0))^{n}}, \qquad q_n \sim \frac{i\Lambda\Gamma(n)}{(i(w-w_0))^{n}} \quad \text{as } n \to \infty. \tag{3.14}$$

For sources and sinks $w - w_0 = \text{const.} \times \log(z - z_0)$. In that case

$$\frac{dw}{dz} = q_0 e^{-i\theta_0} = e^{-i\theta_0} = \text{const.} \times (z - z_0)^{-1} = \text{const.} \times e^{-(w-w_0)}.$$

Hence

$$\theta_0 \sim -i(w - w_0) \tag{3.15}$$

as $w \to w_0$, and in this case there is no singularity in θ_0 and no associated Stokes lines.

3.3. Inner expansion in the vicinity of the complex singularity. Now in the vicinity of the singularity in the complex plane $\log q - i\theta$ is equal to the (regular) expansion of the right-hand side of (2.6), which is evaluated on the real axis, and therefore involves the outer expansion of q and θ away from the singularity. But we know that inserting the expansions for q and θ into the right-hand side simply gives

the outer expansion of $\log q - i\theta$. The right-hand side of this equation in the inner region is therefore simply the inner limit of $\log q - i\theta$. Hence, since $q_0 = 1$ and

$$\theta_0 \sim i\alpha \log(w - w_0) + \text{constant} + \cdots$$

in the vicinity of w_0, where $\alpha = (k-1)/k$, we have

$$\log q - i\theta \sim \alpha \log(w - w_0) + \text{constant} + \cdots, \tag{3.16}$$

$$-2\epsilon q \frac{d\theta}{dw} = q^2 - 1. \tag{3.17}$$

We define the inner variable η by $w = w_0 - \epsilon i\eta$. Then, differentiating (3.16) gives, at leading order in the inner region

$$\frac{q'}{q} - i\theta' = \frac{\alpha}{\eta},$$

where $'$ represents $d/d\eta$. Substituting into (3.17) gives

$$q' + \frac{1}{2}(q^2 - 1) - \frac{\alpha q}{\eta} = 0. \tag{3.18}$$

To determine Λ we need to match the inner limit of (3.14) with the outer limit of (3.18). To this end we expand q as $\eta \to \infty$ as

$$q = \sum_{n=0}^{\infty} \frac{A_n}{\eta^n}, \tag{3.19}$$

giving

$$-(n-1)A_{n-1} - \alpha A_{n-1} + \frac{1}{2}\sum_{m=0}^{n} A_m A_{n-m} = 0,$$

with $A_0 = 1$. Then

$$A_n = (n-1)A_{n-1} + \alpha A_{n-1} - \frac{1}{2}\sum_{m=1}^{n-1} A_{n-m}A_m, \qquad n \geq 1.$$

Writing the outer expansion (3.14) in terms of the inner variable η gives

$$\epsilon^n q_n \sim \frac{i\Lambda\Gamma(n)}{\eta^n} \qquad \text{as } n \to \infty. \tag{3.20}$$

Matching (3.19) and (3.20) gives

$$\Lambda = -i \lim_{n\to\infty} \frac{A_n}{\Gamma(n)}.$$

3.4. Exact solution of the inner problem. In fact, since (3.18) is a Riccati equation we can solve it exactly and determine Λ analytically. We set

$$f = \exp\left(\frac{1}{2}\int q\, d\eta\right), \qquad q = \frac{2f'}{f}$$

to give

$$f'' - \frac{\alpha f'}{\eta} - \frac{f}{4} = 0. \tag{3.21}$$

Since we require $q \to 1$ as $\eta \to +\infty$, the solution is

$$f = \eta^\nu I_\nu(\eta/2), \tag{3.22}$$

where I_ν is the modified Bessel function, and $\nu = 1/2 + \alpha/2$. Hence

$$q = \frac{I_{\nu-1}(\eta/2)}{I_\nu(\eta/2)}. \tag{3.23}$$

Now,

$$I_\nu(z) \sim \frac{e^z}{\sqrt{2\pi z}} \sum_{m=0}^{\infty} \frac{(-1)^m \Gamma(m+\nu+1/2)}{(2z)^m \Gamma(m+1)\Gamma(\nu-m+1/2)} = \frac{e^z}{\sqrt{2\pi z}} \sum_{m=0}^{\infty} \frac{a_m(\nu)\Gamma(m)}{(2z)^m},$$

say. Then the late terms in q satisfy

$$A_n \sim \left(a_\infty(\nu-1) - a_\infty(\nu)\right)\Gamma(n) \qquad \text{as } n \to \infty,$$

where $a_\infty = \lim_{m\to\infty} a_m$. Using the reflection formula

$$\Gamma(-m+\nu+1/2) = -\frac{\pi \operatorname{cosec}(\pi(m-\nu-1/2))}{(m-\nu-1/2)\Gamma(m-\nu-1/2)}$$

and Stirling's formula we find that

$$a_\infty(\nu) = \frac{\cos \pi\nu}{\pi},$$

so that

$$A_n \sim -\frac{2\cos\pi\nu}{\pi}\Gamma(n) = \frac{2\sin(\pi\alpha/2)}{\pi}\Gamma(n).$$

Hence

$$\Lambda = -\frac{2i\sin(\pi\alpha/2)}{\pi}. \tag{3.24}$$

This completes the determination of the late terms in the asymptotic expansion of q and θ. The next step is to optimally truncate the expansion and examine the switching on of exponentially small terms across Stokes lines.

4. Stokes line smoothing. We keep the analysis here brief since it is similar to that in [5]. We begin by truncating the expansion after N terms, so that

$$\theta = \sum_{n=0}^{N-1} \epsilon^n \theta_n + R_N, \qquad q = \sum_{n=0}^{N-1} \epsilon^n q_n + S_N.$$

Then the argument leading to (3.10) implies $S_N \sim iR_N$, which in (2.7) gives

$$iR_N + \epsilon \frac{dR_N}{dw} + \cdots \sim i\epsilon^N \theta_N + \cdots \tag{4.1}$$

as $N \to \infty$ and $\epsilon \to 0$. The homogeneous version of this equation has a solution

$$R_N \sim e^{-iw/\epsilon}, \tag{4.2}$$

corresponding to capillary waves on the free surface. Following Dingle [9] we expect there to be Stokes lines whenever successive terms in the expansion of θ have the same phase, i.e., when χ is real and positive, so that $w - w_0$ is negative imaginary. Hence there will be Stokes lines down parallel to the imaginary axis from the singularities in the upper half w-plane. We will show that a multiple of (4.2) is switched on across these Stokes lines. We define the Stokes multiplier A by setting

$$R_N = Ae^{-iw/\epsilon},$$

giving

$$\epsilon e^{-iw/\epsilon}\frac{dA}{dw} \sim i\epsilon^N\theta_N \sim \frac{i\epsilon^N\Lambda\Gamma(N)}{(i(w-w_0))^N}. \tag{4.3}$$

Now the right-hand side of (4.3) is minimal for $N \sim |w - w_0|/\epsilon$. Hence we let $N = |w - w_0|/\epsilon + \rho$, where ρ is bounded as $\epsilon \to 0$. Then, since N is a function of $|w - w_0|$ only, following [5, 15] we write $w - w_0 = -ire^{i\vartheta}$ and write

$$\frac{d}{dw} = \frac{e^{-i\vartheta}}{r}\frac{d}{d\vartheta}.$$

Then, as $\epsilon \to 0$,

$$\begin{aligned}\epsilon e^{-re^{i\vartheta}/\epsilon}\frac{e^{-i\vartheta}}{r}\frac{dA}{d\vartheta} &\sim \frac{i\epsilon^N\Lambda\sqrt{2\pi}e^{-N}N^{N-1/2}}{r^N e^{iN\vartheta}}\\ &= \frac{i\epsilon^{(r/\epsilon+\rho)}\Lambda\sqrt{2\pi}e^{-(r/\epsilon+\rho)}(r/\epsilon+\rho)^{(r/\epsilon+\rho-1/2)}}{r^{(r/\epsilon+\rho)}e^{i\vartheta(r/\epsilon+\rho)}}\\ &\sim \frac{i\sqrt{2\pi}\,\Lambda\epsilon^{1/2}e^{-r/\epsilon}}{r^{1/2}e^{i\vartheta(r/\epsilon+\rho)}}.\end{aligned}$$

Hence

$$\frac{dA}{d\vartheta} \sim \frac{i\sqrt{2\pi}\,\Lambda r^{1/2}e^{i\vartheta}e^{-r/\epsilon}e^{re^{i\vartheta}/\epsilon}}{\epsilon^{1/2}e^{i\vartheta(r/\epsilon+\rho)}}.$$

Now, the right-hand side is exponentially small except near the Stokes line $\vartheta = 0$. Thus there is a rapid variation in A at this point, corresponding to the switching on of our subdominant exponential. To examine this transition we introduce the local scaling $\vartheta = \delta\bar{\vartheta}$, giving

$$\frac{dA}{d\bar{\vartheta}} \sim \frac{i\delta\sqrt{2\pi}\,\Lambda r^{1/2}e^{-r\delta^2\bar{\vartheta}^2/(2\epsilon)}}{\epsilon^{1/2}}.$$

We see that the correct scaling is $\delta = \epsilon^{1/2}$, giving

$$\frac{dA}{d\bar{\vartheta}} \sim i\sqrt{2\pi}\,\Lambda r^{1/2}e^{-r\bar{\vartheta}^2/2}.$$

Hence

$$A = a + i\sqrt{2\pi}\,\Lambda\int_{-\infty}^{\bar{\vartheta}\sqrt{r}} e^{-t^2/2}\,dt,$$

and we have the usual error function smoothing of the Stokes discontinuity [2]. Matching with the outer solution away from the Stokes line we find there is a jump in A given by

$$A(\vartheta = 0-) - A(\vartheta = 0+) = 2\pi i \Lambda. \tag{4.4}$$

In summary, there are Stokes lines down parallel to the imaginary axis from singularities in the upper half w-plane across which

$$2\pi i \Lambda \exp\left(-\frac{i(w - w_0)}{\epsilon}\right) \tag{4.5}$$

is switched on. Throughout we have been working in the upper half ζ-plane, corresponding to the upper half w-plane. If we were to instead analytically continue into the lower half ζ-plane, we would find that there are Stokes lines up parallel to the imaginary axis from singularities in the lower half w-plane. Since the singularities off the real axis appear in complex conjugate pairs, and since we know that the solution on the real axis must be real, we find that where the Stokes lines meet the free boundary (4.5) plus its complex conjugate must be turned on.

Combining this with our expression (3.24) for Λ we find that if $w_0 = \phi_0 + i\psi_0$, then the capillary waves turned on across the Stokes line are given by

$$R_N \sim 8 \sin\left(\frac{\pi\alpha}{2}\right) e^{-\psi_0/\epsilon} \cos\left(\frac{(\phi - \phi_0)}{\epsilon}\right).$$

This expression gives the oscillations in θ, the angle the tangent to the free surface makes with the x-axis. If we are interested instead in the height of the waves, then we need to integrate with respect to ϕ to give

$$8\epsilon \sin\left(\frac{\pi\alpha}{2}\right) e^{-\psi_0/\epsilon} \sin\left(\frac{(\phi - \phi_0)}{\epsilon}\right).$$

Thus the amplitude of the capillary waves generated is

$$8\epsilon \sin(\pi\alpha/2) e^{-\psi_0/\epsilon}. \tag{4.6}$$

Before we go on to consider some specific examples of flows, we make some general comments about the results so far and formula (4.6). First, we note that the strength of the exponential factor in the amplitude is determined by the difference in the value of the streamfunction on the free boundary and at the singularity (since we have set $\psi = 0$ on the free boundary), which is the flux of fluid between the two streamlines. The nearer the submerged singularities are to the free boundary the stronger the capillary waves will be. If there are two singularities with different values of ψ, the waves generated by the closer one will exponentially dominate those generated by the farther one.

Second, we note that the Stokes lines, given by $i(w - w_0)$ real and positive, correspond to constant real part of $w - w_0$; i.e., the Stokes line meets the free boundary at the point where the equipotential from the singularity in the flow meets the free boundary.

Thus we are able to say a lot about the capillary waves on the free surface even when we know very little about the unperturbed flow. In the next section we consider a specific flow and compare our asymptotic results to a direct numerical simulation of the full problem. Then, in section 6, we consider some more general examples of potential flows.

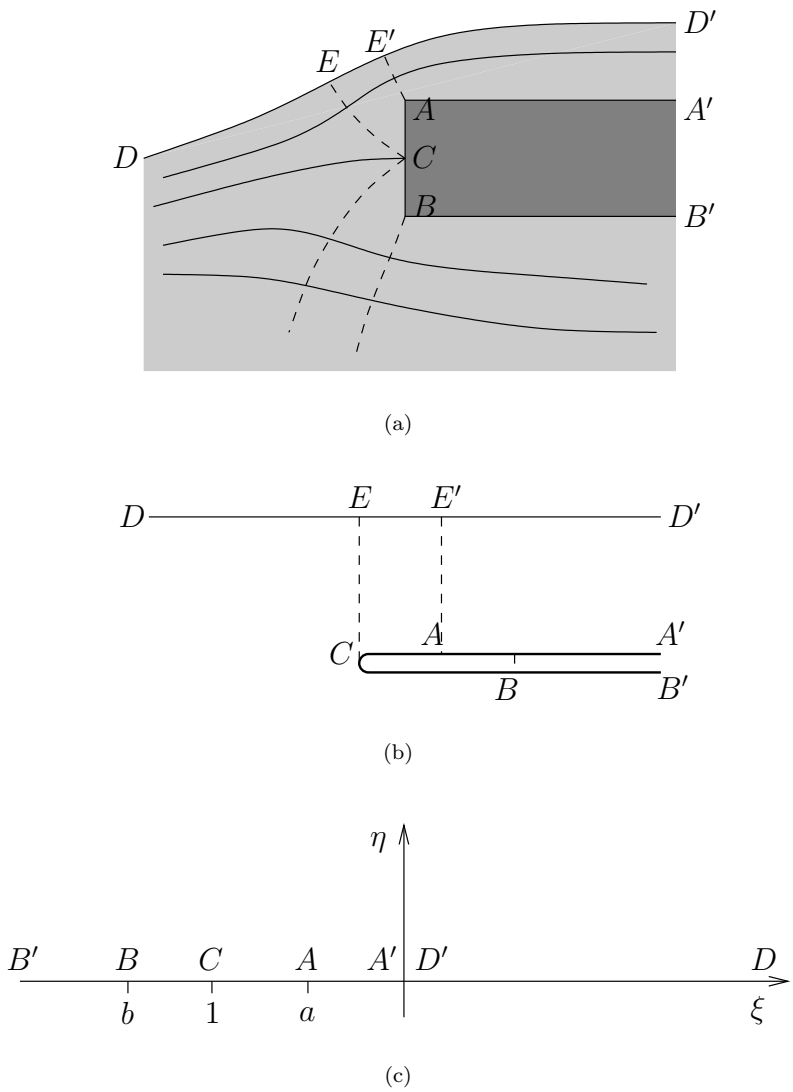

FIG. 1. (a) *A schematic diagram of a polygonal ploughing flow.* (b) *The complex potential plane. The stagnation point C is a square-root branch point for $z(w)$. There are also singularities in θ_0 at the corners A and B. There are Stokes lines (dashed) meeting the free boundary originating at A and C.* (c) *The ζ-plane.*

5. A polygonal ploughing flow. We consider in detail the case of the ploughing flow shown in Figure 1; in particular, we will compare the asymptotic results with a direct numerical simulation of the full problem. The asymptotic and numerical results are presented in sections 5.1 and 5.2, respectively.

5.1. Asymptotic results. For the flow shown in Figure 1(a), the fluid region corresponds to a region in the lower half w-plane, shown in Figure 1(b). Let us normalize lengths so that the height of the fluid above the plough at $s = +\infty$ is π.

Then the map from the w-plane into the upper half ζ-plane is given by

$$w = -\zeta - \log \zeta. \tag{5.1}$$

The free boundary is mapped to $0 < \zeta < \infty$, the stagnation point to $\zeta = -1$, and the corners of the step to $\zeta = -a$ and $\zeta = -b$, respectively, with $0 < a < 1 < b$. As we mentioned in section 2, the analyticity of $\log q - i\theta$ in the upper half ζ-plane implies that for ζ real

$$\log q = -\frac{1}{\pi} \fint_{-\infty}^{\infty} \frac{\theta(\zeta')\, d\zeta'}{\zeta' - \zeta}. \tag{5.2}$$

Now, since the position of the fixed boundary is known, we have

$$\theta = \begin{cases} 0 & -\infty < \zeta < -b, \\ -\frac{\pi}{2} & -b < \zeta < -1, \\ \frac{\pi}{2} & -1 < \zeta < -a, \\ 0 & -a < \zeta < 0. \end{cases}$$

Then, since

$$\frac{dw}{d\zeta} = \frac{1+\zeta}{\zeta},$$

our system is

$$q^2 - 1 = -2\epsilon q \frac{\zeta}{1+\zeta} \frac{d\theta}{d\zeta}, \tag{5.3}$$

$$\log q = \frac{1}{2} \log \left(\frac{(1+\zeta)^2}{(a+\zeta)(b+\zeta)} \right) - \frac{1}{\pi} \fint_0^{\infty} \frac{\theta(\zeta')\, d\zeta'}{\zeta' - \zeta}. \tag{5.4}$$

One relationship between the two free parameters a and b is determined by the condition that the free boundary is asymptotically flat far upstream. The remaining free parameter is determined by the height of the plough. We will take a as the free parameter giving ploughs of different heights and determine b from the condition of a flat upstream free surface.

Then the leading-order solution satisfies

$$q_0 = 1, \tag{5.5}$$

$$0 = \frac{1}{2} \log \left(\frac{(1+\zeta)^2}{(a+\zeta)(b_0+\zeta)} \right) - \frac{1}{\pi} \fint_0^{\infty} \frac{\theta_0(\zeta')\, d\zeta'}{\zeta' - \zeta}, \tag{5.6}$$

with solution

$$\theta_0 = -2 \tan^{-1}(\zeta)^{1/2} + \tan^{-1}(\zeta/a)^{1/2} + \tan^{-1}(\zeta/b_0)^{1/2}. \tag{5.7}$$

To ensure that the free boundary is asymptotically flat far upstream, we require

$$a^{1/2} + b_0^{1/2} = 2, \tag{5.8}$$

so that $\theta_0 = O(\zeta^{-3/2})$ as $\zeta \to \infty$. The solution (5.7), (5.8) was previously derived in [16].

The relevant singularities in θ_0 from the point of view of capillary waves are the stagnation point $\zeta = -1$ and the corner $\zeta = -a$; it is clear from Figure 1 that the equipotential from the corner $\zeta = -b_0$ does not meet the free boundary. For the stagnation point $w_0 = 1 + i\pi$, $k = 2$, $\alpha = 1/2$, while for the corner $w_0 = a - \log a + i\pi$, $k = 2/3$, $\alpha = -1/2$. Since our analysis gives only the jump in the amplitude of capillary waves on the free surface, to compare with numerical results we impose that there are no capillary waves far upstream and examine the behavior of the free surface far downstream. Then the capillary waves present as $s \to \infty$ are given by the superposition of those generated at each Stokes line, namely,

$$\begin{aligned}\theta &\sim -4\sqrt{2}e^{-\pi/\epsilon}\cos\left(\frac{(1-\phi)}{\epsilon}\right) + 4\sqrt{2}e^{-\pi/\epsilon}\cos\left(\frac{(a-\log a-\phi)}{\epsilon}\right)\\ &= 4\sqrt{2}e^{-\pi/\epsilon}\mathrm{Re}\left(\left(e^{i(a-\log a)/\epsilon} - e^{i/\epsilon}\right)e^{-i\phi/\epsilon}\right),\end{aligned}$$

which corresponds to

$$y \sim y_0 - 4\sqrt{2}\epsilon e^{-\pi/\epsilon}\mathrm{Im}\left(\left(e^{i(a-\log a)/\epsilon} - e^{i/\epsilon}\right)e^{-i\phi/\epsilon}\right).$$

Hence the amplitude of the wave train at infinity is

$$4\sqrt{2}\epsilon e^{-\pi/\epsilon}\left|e^{i(a-\log a)/\epsilon} - e^{i/\epsilon}\right|. \tag{5.9}$$

As $a \to 0$ the factor $|e^{i(a-\log a)/\epsilon} - e^{i/\epsilon}|$ vanishes infinitely often, as the waves from the two singularities move in and out of phase. When the two wave trains are out of phase, the waves that are turned on at the first Stokes line are effectively turned off at the second, and there is a finite section of the free boundary on which capillary waves are present. This cancellation can occur because the amplitude of the waves generated by the stagnation point and the corner are exactly equal at leading order, since

$$\left|\sin\left(\frac{\pi\alpha_{corner}}{2}\right)\right| = \left|\sin\left(\frac{\pi\alpha_{stagnation}}{2}\right)\right|.$$

Although such a situation would seem to be very special, we will see in section 6 that there are many examples of potential flows where two singularities generate waves of exactly the same amplitude, and we have the possibility of a finite section of the free boundary containing capillary waves.

The limit $a \to 0$ is a singular one since the stagnation point disappears to infinity but the capillary waves it generates are still felt, and the difference in ϕ at the stagnation point and the corner determines the phase difference of the two trains of waves. The case $a = 0$ corresponds to flow around a corner, shown in Figure 2. In this case there is no stagnation point and only one set of waves present, with amplitude

$$4\sqrt{2}\epsilon e^{-\pi/\epsilon}. \tag{5.10}$$

In the next section we describe our numerical scheme and compare these asymptotic results to a direct numerical simulation of the full problem.

5.2. Numerical results. Following Tuck and Vanden-Broeck [16], we introduce the equally spaced mesh points in ϕ,

$$\phi_I = X_- + \left(\frac{I-1}{N-1}\right)(X_+ - X_-), \quad I = 1, \ldots, N, \tag{5.11}$$

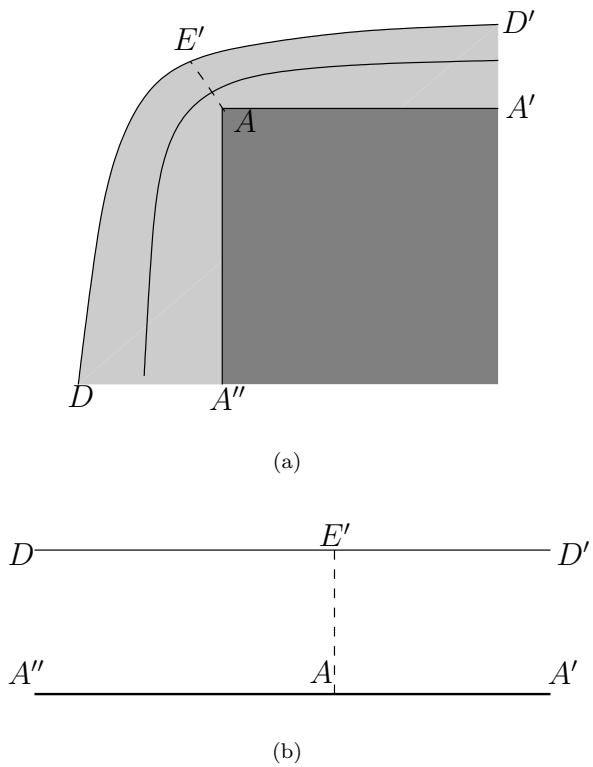

FIG. 2. (a) *A schematic diagram of flow around a corner.* (b) *The complex potential plane. The only singularity in θ_0 is at the corner A. There is one Stokes line (dashed) meeting the free boundary, originating at A.*

and the corresponding unknowns,

$$\theta_I = \theta[\zeta(\phi_I)], \quad I = 1, \ldots, N. \tag{5.12}$$

For a given value of ϕ, $\zeta(\phi)$ is defined by setting $\psi = 0$ in (5.1) and solving the resulting transcendental equation by Newton's method.

Writing $\tau = \log q$, we evaluate the values τ_I^M of $\tau[\zeta(\phi)]$ at the midpoints

$$\phi_I^M = \frac{\phi_I + \phi_{I+1}}{2}, \quad I = 1, \ldots, N-1, \tag{5.13}$$

by applying the trapezoidal rule to the integral in (5.4) with a summation over the points ϕ_I. The symmetry of the quadrature and of the distribution of mesh points enabled us to evaluate the Cauchy principal value as if it were an ordinary integral.

We evaluate the values of $\theta[\zeta(\phi)]$ at the midpoints ϕ_I^M by interpolation formulas We now satisfy (2.5) at the midpoints ϕ_I^M, $I = 1, \ldots, N-1$. For given values of ϵ and a, this yields $N-1$ nonlinear algebraic equations for the $N+1$ unknowns θ_I and b. Two more equations are obtained by imposing $\theta_1 = \theta_2 = \theta_3$. This forces the free surface to be flat far upstream. This system of $N+1$ equations with $N+1$ unknowns is solved by Newton's method. For ϵ small, the exact solution for $\epsilon = 0$ is chosen as an initial guess. For larger values of ϵ a continuation method is used; i.e., a

converged solution is used as an initial guess to compute a solution for a larger value of ϵ. Most calculations were performed with $N = 1500$, $X_- = -81$, and $X_+ = 54$. We repeated some of the calculations with larger values of N, X_+, and $|X_-|$ and checked that all the results presented are independent of the values of these parameters within graphical accuracy.

A typical free surface profile is shown in Figure 3. As ϵ increases, the amplitude of the waves increase and the profiles approach the limiting configuration with a trapped bubble at the trough predicted by the exact solutions of Crapper [7] and Kinnersley [13].

In Figure 4 we show a comparison of the asymptotic and numerical values of the log of the amplitude of the waves at infinity as ϵ varies for $a = 0.26644$. In Figure 5 we show a comparison of the asymptotic and numerical values of the amplitude of the waves at infinity as a varies for $\epsilon = 0.4$. We see that the asymptotic solution is remarkably accurate, even at relatively large values of ϵ.

We found that larger and larger values of N were needed to compute accurate solutions as a was decreased below 0.15, and we are unable to extend the numerical results to the predicted first cancellation between the two asymptotic wave trains. However, the numerical results do confirm the maximum in the amplitude of the waves predicted by the asymptotic solution.

For the limiting case $a = 0$ corresponding to flow around a corner we derived a separate numerical scheme. The flow configurations in the physical plane and in the complex potential plane are illustrated in Figure 2. We map the complex potential of Figure 2(b) into the lower half of the $\alpha + i\beta$ plane by the transformation

$$\alpha + i\beta = e^{-(\phi + i\psi)}. \tag{5.14}$$

The free surface is mapped on the negative α-axis and the corner on the positive α-axis.

We denote by $\tau_\infty - i\theta_\infty$ the free streamline solution corresponding to $\epsilon = 0$ (i.e., no surface tension). Next we apply the Cauchy integral formula to the function

$$\tau - \tau_\infty - i(\theta - \theta_\infty) \tag{5.15}$$

with a contour consisting of the α-axis and a semicircle of arbitrary large radius in the lower $\alpha + i\beta$-plane. This yields

$$\tau(\alpha) = \frac{1}{\pi} \int_{-\infty}^{0} \frac{\theta(\bar{\alpha}) - \theta_\infty(\bar{\alpha})}{\bar{\alpha} - \alpha} d\bar{\alpha}. \tag{5.16}$$

In (5.16), we used the properties $\theta - \theta_\infty = 0$ on the positive α-axis and $\tau_\infty = 0$ on the free surface $\alpha > 0$. The integral in (5.16) is a Cauchy principal value. The numerical procedure then follows the one described at the beginning of this section with (5.4) replaced by (5.16) and $\zeta(\phi)$ by $\alpha(\phi) = -e^{-\phi}$.

A typical free surface profile is shown in Figure 6. In Figure 7 we show a comparison of the asymptotic and numerical values of the log of the amplitude of the waves at infinity as ϵ varies for $a = 0$.

6. Other examples. In this section we consider the implications of our analysis for some general potential flows.

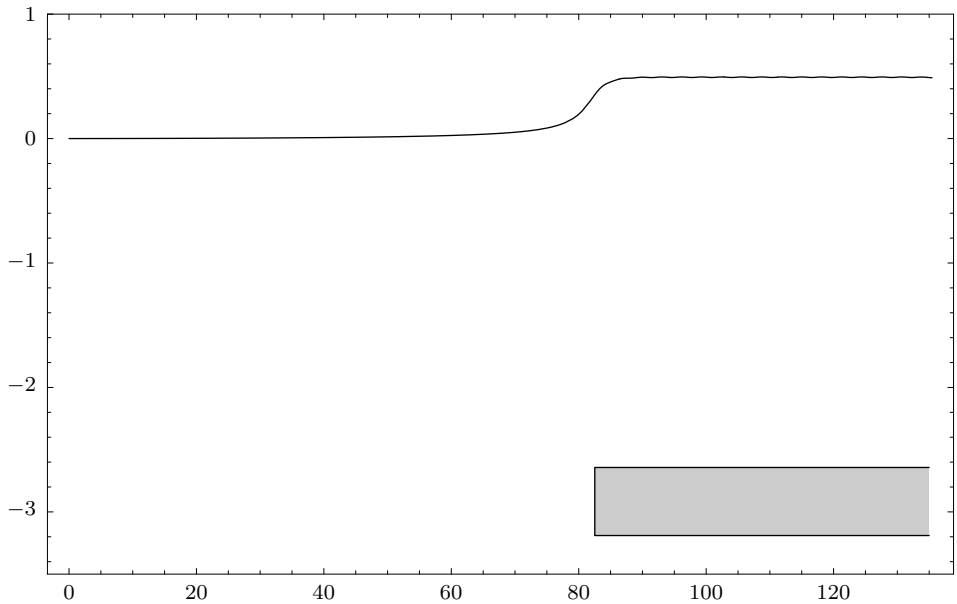

(a)

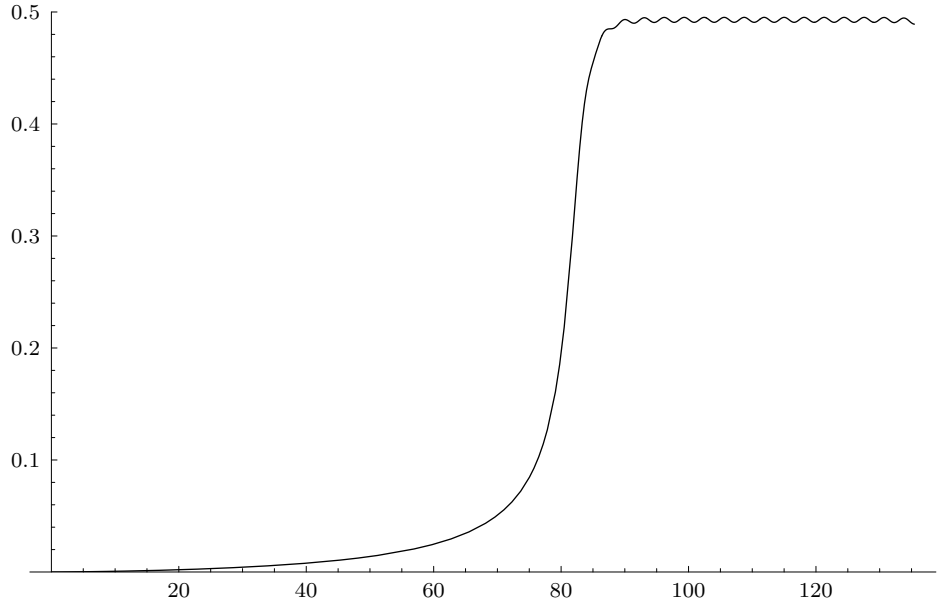

(b)

FIG. 3. (a) *The flow region for* $\epsilon = 0.5$, $a = 0.5$ *showing the free surface and the position of the plough.* (b) *A close-up of the free surface showing the wave train generated by the plough.*

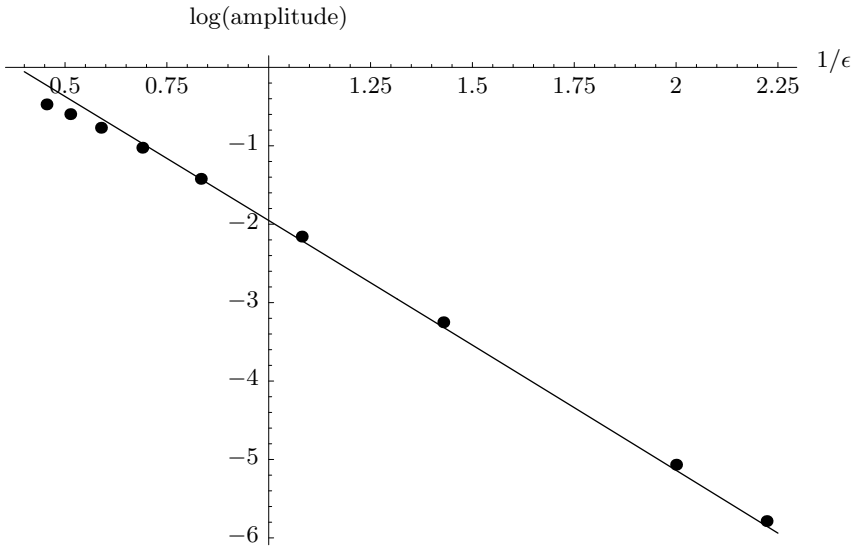

FIG. 4. *The logarithm of the amplitude of the capillary wave train at infinity as a function of* $1/\epsilon$ *for* $a = 0.26644$. *The solid curve is the asymptotic value* (5.9). *The points are the results of the numerical simulation.*

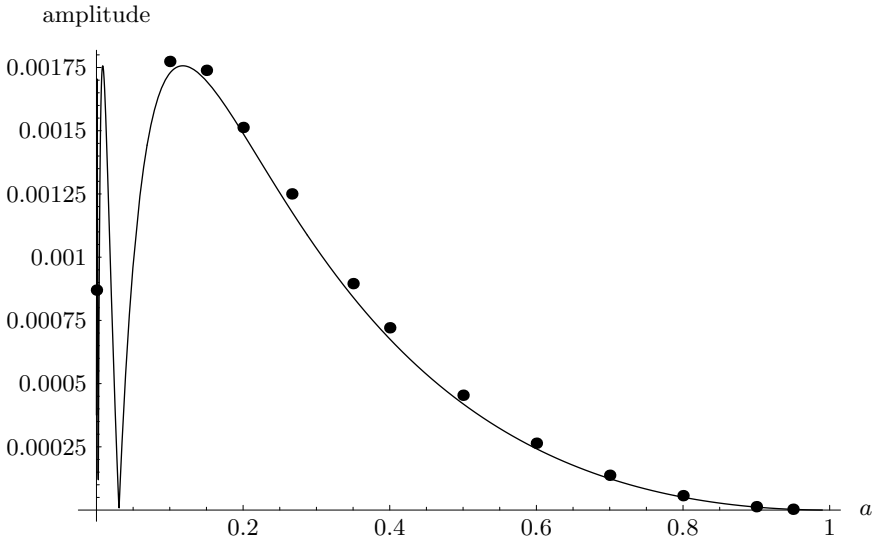

FIG. 5. *The amplitude of the capillary wave train at infinity as a function of* a, *the parameter in the problem which determines the height of the plough relative to the height of water above it, for* $\epsilon = 0.4$. *The solid curve is the asymptotic value* (5.9). *The points are the results of the numerical simulation. The asymptotic result predicts that the amplitude should vanish (to leading order) for a discrete set of values of* a *accumulating at zero. The numerical simulation becomes very difficult for small values of* a, *although we have been able to see the local maximum in the amplitude. The numerical calculation at* $a = 0$ *is much easier; since in this case there is only one wave train the amplitude is half the value of the maximum.*

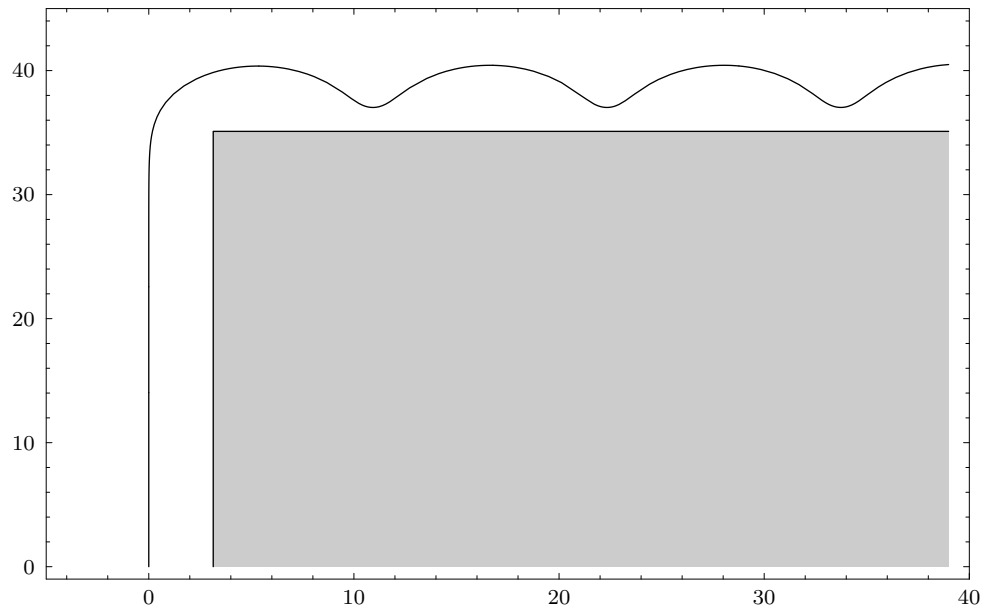

FIG. 6. *The free surface for flow around a corner with* $\epsilon = 2.1$.

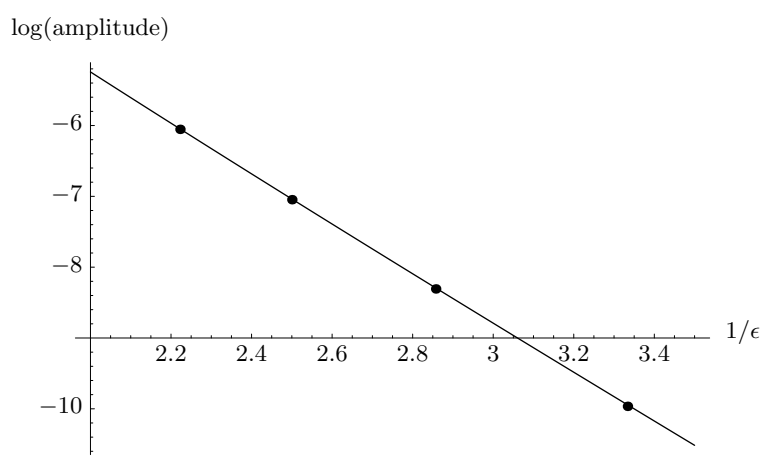

FIG. 7. *The logarithm of the amplitude of the capillary wave train at infinity as a function of* $1/\epsilon$ *for the flow round a corner* ($a = 0$)*. The solid curve is the asymptotic value* (5.10)*. The points are the results of the numerical simulation.*

6.1. Ploughing flows. A general ploughing flow is illustrated in Figure 8. The relevant singularities in θ_0 will be the stagnation point on the plough and any corners it may have. Since these all lie on the same streamline they have the same value of ψ_0 and hence the same exponential factor in the amplitude of the capillary waves generated. To determine where on the free surface the waves begin we simply follow

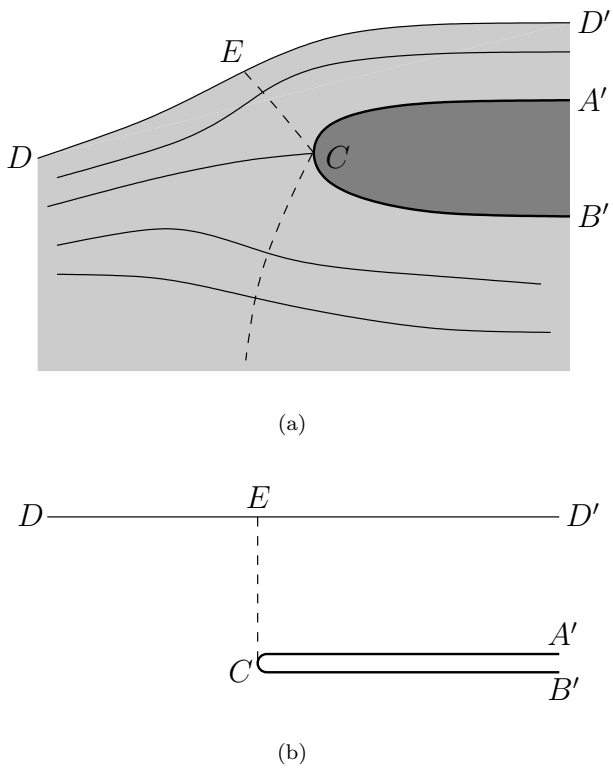

FIG. 8. (a) *A schematic diagram of a general ploughing flow.* (b) *The complex potential plane. The stagnation point C is a square-root branch point of $z(w)$. There is only one Stokes line (dashed) meeting the free boundary, which originates at C.*

the equipotential from each singularity until it meets the free surface. Note that there are two such equipotentials from the stagnation point, but only one meets the free surface.

If the plough is polygonal, these will be the only singularities in the flow field. For general ploughs, though, when we analytically continue the solution into the plough we will encounter further singularities, which will also generate capillary waves. However, these will all have a value of ψ greater than that on the boundary of the plough, and will therefore generate waves which are exponentially subdominant to those generated by singularities on the plough itself.

The wave train proceeding to infinity will be the superposition of those generated at each singularity. If the plough is analytic, the only relevant singularity is the stagnation point, and the amplitude of waves at infinity will be

$$4\sqrt{2}\epsilon e^{-\psi_0/\epsilon}.$$

6.2. Flow over a rough boundary. For flow over a general smooth surface we need to analytically continue outside the flow domain until we meet the first singularity. Generically there will be one such singularity and it will generate a train of capillary waves. (Occasionally we meet more than one singularity with the same value of ψ; for example, any streamline in Figure 1 may be taken as the boundary

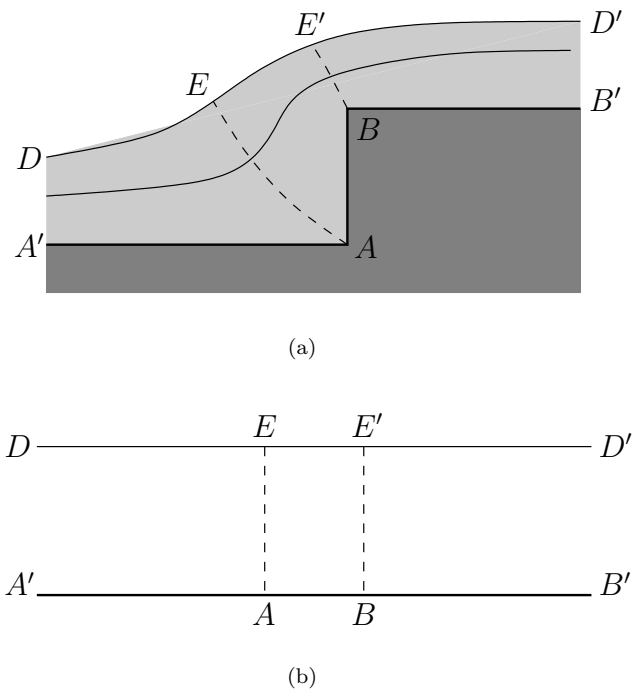

FIG. 9. (a) *A schematic diagram of flow over a step.* (b) *The complex potential plane. There are two Stokes lines (dashed) meeting the free boundary, originating at the corners A and B.*

of a flow, the analytic continuation of which will lead to the corner and stagnation point singularities.) If the surface is not smooth, then we know that the nearest singularities are those on the surface. For example, for flow over the step shown in Figure 9 there are two relevant singularities, corresponding to the two corners. Since $k = 2/3$, $\alpha = -1/2$ for one corner, and $k = 2$, $\alpha = 1/2$ for the other, the waves generated by both singularities have the same amplitude and there is again, therefore, the possibility that they are exactly out of phase and cancel out. Thus there is a discrete set of step heights (accumulating at infinity) for which there is a bounded region of capillary waves on the free surface.

6.3. Flow past a submerged object. For flow past a smooth object (as shown in Figure 10, for example) there will in general be two singularities on the surface of the object corresponding to the leading and trailing stagnation points. These both have $k = 2/3$, $\alpha = -1/2$ so that there is the possibility that the wave trains again cancel, which they will do for a discrete set of values of ϵ.

If the object also has corners, then we have to take into account the waves generated by these singularities, also.

If there is circulation about the object, then the two stagnation points may merge and eventually detach, as shown in Figure 11. Then there is only one singularity, but there are two equipotential lines from it which meet the free surface, so that there will still be two wave trains. Whether these are out of phase or not depends on the "depth" of the stagnation point, so that in this case there is a discrete set of values for the circulation for which there are bounded waves on the free surface.

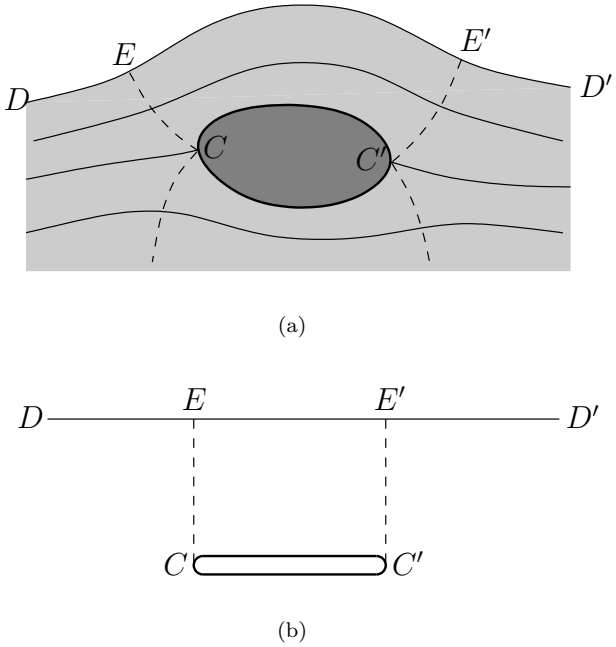

FIG. 10. (a) *A schematic diagram of flow around a submerged obstacle.* (b) *The complex potential plane. The stagnation points C and C' are square-root branch points of $z(w)$. There are two Stokes lines (dashed) meeting the free boundary, originating from these stagnation points.*

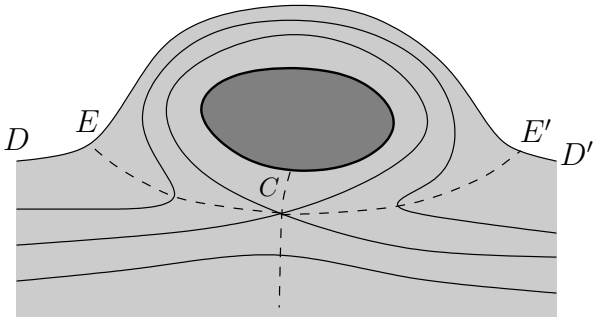

FIG. 11. *A schematic diagram of flow around a submerged obstacle with large circulation. The stagnation points have merged into one which has left the boundary of the obstacle. There are still two Stokes lines (dashed) meeting the free boundary, both originating from this one stagnation point.*

6.4. Impinging jets. Figure 12 shows equal and opposite impinging jets (or equivalently a jet impinging normally on a plane wall). The only singularity is the stagnation point, and the equipotentials from it meet each of the free boundaries once, so that each of the incoming jets will have a train of capillary waves on each side. This easily generalizes to unequal and/or obliquely impinging jets.

6.5. Source beneath a free surface. In [12] the problem of a source lying beneath a free surface and above a flat horizontal bottom is considered, as shown in Figure 13. The free surface has a discontinuous gradient, near which an inner

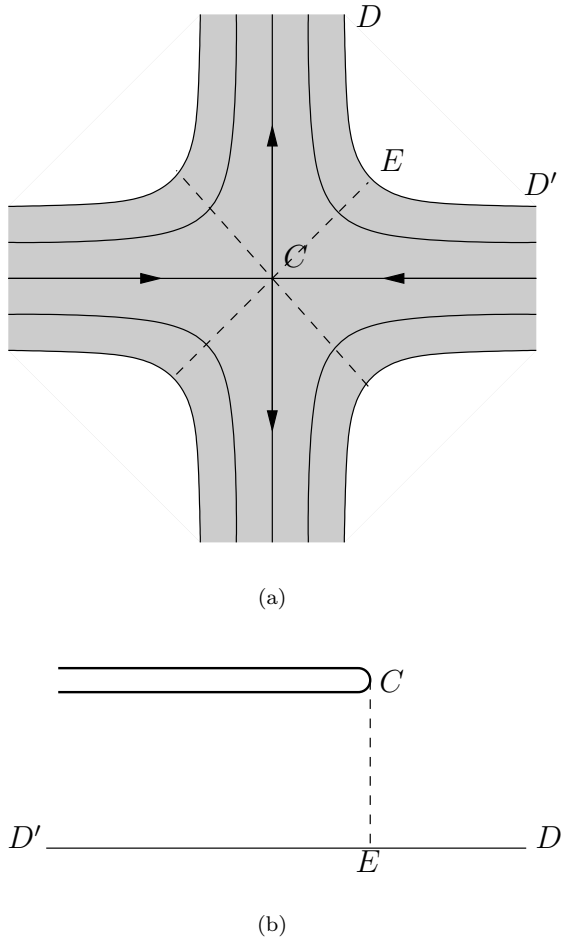

FIG. 12. (a) *A schematic diagram of impinging equal and opposite jets.* (b) *The complex potential plane. The stagnation point C is a square-root branch point of $z(w)$. There is one Stokes line (dashed) from this point meeting each of the free boundaries.*

problem would need to be solved when a small amount of surface tension is introduced. However, there is also a stagnation point on the lower surface, which can produce additional capillary waves on the free surface.

If the source is sufficiently close to the free surface, then the equipotential from the stagnation point meets the free boundary (in two places, one either side of the cusp), and exponentially small capillary waves will be generated at these points. However, if the source is close to the lower boundary, then the equipotential from the stagnation point meets the streamline DC on the section $D'C$, so that capillary waves are not generated on the free boundary in this case.

6.6. Gliding and planing. A typical gliding or planing flow is shown in Figure 14. In this case the relevant singularities are the stagnation point C and the ends of the plate A and B. No equipotential from any of these meets the free boundaries $A'A$ and $B'B$ (although there is an inner problem in the vicinity of A and B which

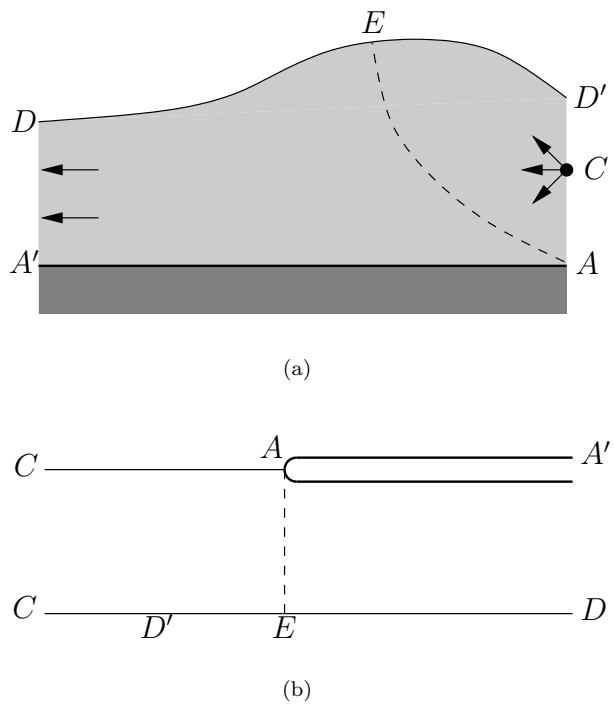

FIG. 13. (a) *A schematic diagram of a source above a flat horizontal boundary and beneath a free surface. Only the left half of the physical plane is shown.* (b) *The complex potential plane. The source C lies at infinity, while the stagnation point A' is a square-root branch point of $z(w)$. There is one Stokes line (dashed) from this point meeting the free boundary.*

may generate waves on these free boundaries). However, equipotentials from A and C meet the free boundary $D'D$ at E' and E, respectively. Hence there will be two sets of capillary waves on this free surface, one generated at E' and one generated at E.

However, the flow separation point A is a type of flow singularity that we have not yet considered. The behavior in the vicinity of A is more tricky than that near a stagnation point or corner, but it is still not difficult to show that

$$\theta_0 \sim \text{const.} + \text{const.}(w - w_0)^{1/2} \tag{6.1}$$

as $w \to w_0$. This means that for these singularities $\gamma = -1/2$ rather than zero. The analysis in section 4 is modified in an obvious way (see [5] for the details), and the result is that

$$2\pi i \Lambda \epsilon^{1/2} \exp\left(-\frac{i(w - w_0)}{\epsilon}\right) \tag{6.2}$$

is switched on across Stokes lines in the upper half plane. Thus the capillary waves generated are smaller in amplitude by a factor of $\epsilon^{1/2}$ than those generated at the stagnation point.

The inner problem in the vicinity of w_0 on the free boundary to determine Λ is

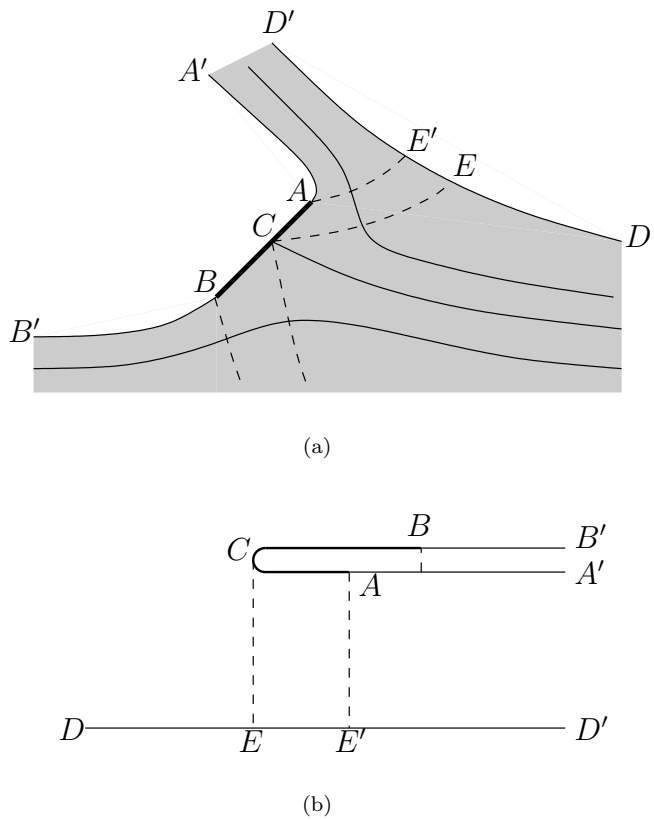

FIG. 14. (a) *A schematic diagram of a gliding flow.* (b) *The complex potential plane. The stagnation point C is a square-root branch point of w. There are Stokes lines (dashed) meeting the free boundary, originating at A and C.*

also modified. The corresponding analysis is given in the appendix, and the result is

$$\Lambda = \frac{\beta e^{-5i\pi/4}}{2\sqrt{\pi}},$$

where

$$\theta_0 \sim \text{const.} + \beta(w - w_0)^{1/2} + \cdots$$

as $w \to w_0$.

7. Conclusion. We have employed recently developed techniques in asymptotics beyond all orders to examine the problem of exponentially small capillary waves on potential flows with small surface tension in the absence of gravity. Much of the theory can be worked out analytically, and the results are pleasingly simple.

We find that waves will be generated whenever the equipotential from a singularity in the flow (such as a corner or stagnation point) meets the free surface. Our analysis gives the jump in the amplitude of the waves as this equipotential is crossed; to determine on which section of the free boundary they are present, the standard

radiation condition needs to be used. The jump in amplitude of the waves is found to be of the form

$$C\epsilon^n e^{-\psi_0/\epsilon}, \tag{7.1}$$

where ψ_0 is the modulus of the difference between the streamfunction on the free surface and at the singularity (i.e., the flux of fluid between these streamlines, since the unperturbed skin speed is normalized to unity), and ϵ is the surface tension parameter. The algebraic factor ϵ^n depends in a simple way on the type of singularity; corners and stagnation points have $n = 1$, while separation points have $n = 3/2$. Finally, the constant C can also be calculated simply; for corners and stagnation points $C = 8\sin(\pi\alpha/2)$, where $dw/dz \propto (w - w_0)^\alpha$ locally. Typically, for a stagnation point $\alpha = 1/2$, while for flow around a corner $\alpha = 1 - \beta/\pi$, where β is the interior (i.e., in the fluid) angle of the corner.

For flows which have singularities in the physical domain (flows with stagnation points or flows around polygonal objects) the relevant singularities are easy to determine. Flows with no singularities in the physical domain must be analytically continued to find the nearest singularity outside the flow domain.

An intriguing possibility, which seems to be realized in many of the flows we have examined, is that there are two Stokes lines meeting the free boundary with a bounded region containing capillary waves between them—the waves turned on at the first Stokes line are effectively turned off at the second.

We have compared our asymptotic results with a direct numerical simulation for a simple ploughing flow and for flow around a right-angled corner. In both cases the results are surprisingly accurate, even at values of ϵ as high as 1.5.

Finally, we have a word of warning when determining the position of singularities, especially when this involves analytically continuing outside the flow region. Because of the exponential dependence of the waves on the value of the complex potential at the singularity, an order-ϵ perturbation to the position of the singularity produces and order-one perturbation to the waves. If this perturbation is in ψ, the amplitude of the wave is perturbed by an order one amount, while if it is in ϕ, the phase of the waves is perturbed by an order one amount. This is the reason we chose a as our control parameter in the example of section 5; if we had used b to control the height of the plough it would have been much harder to compare to the numerical solution, since we would need to know a to order ϵ. However, having said this, for many problems (such as those we have considered) the positions of the singularities are determined exactly (or at least the value of ψ at the singularity is), since they lie at corners or stagnation points on a submerged object.

Appendix A. Inner expansion in the vicinity of the complex singularity generated by flow separation.

As in section 3.3, in the vicinity of the singularity in the complex plane the right-hand side of (2.6) in the inner region is simply the inner limit of $\log q - i\theta$. Hence, since $q_0 = 1$ on the free boundary, and

$$\theta_0 \sim \text{const.} + \beta(w - w_0)^{1/2} + \cdots,$$

say, in the vicinity of w_0, we have

$$\log q - i\theta \sim -i\beta(w - w_0)^{1/2} + \text{const.} + \cdots, \tag{A.1}$$

$$-2\epsilon q \frac{d\theta}{dw} = q^2 - 1. \tag{A.2}$$

We define the inner variable η as before by $w = w_0 - \epsilon i\eta$. Then, differentiating (A.1) gives

$$\frac{q'}{q} - i\theta' = \frac{\beta e^{-3i\pi/4}\epsilon^{1/2}}{2\eta^{1/2}},$$

where $'$ represents $d/d\eta$. Substituting into (A.2) gives

$$q' + \frac{1}{2}(q^2 - 1) - \frac{\beta e^{-3i\pi/4}\epsilon^{1/2} q}{2\eta^{1/2}} = 0. \tag{A.3}$$

Now the correct scaling for q is

$$q = 1 + \frac{\beta\epsilon^{1/2} e^{-3i\pi/4}\bar{q}}{2}, \tag{A.4}$$

giving to leading order

$$\bar{q}' + \bar{q} - \frac{1}{\eta^{1/2}} = 0. \tag{A.5}$$

Thus the relevant inner problem for q is in fact linear, unlike in section 3.3 where it was nonlinear. This is because the singularity generated by flow separation is not in the leading-order term in $z(w)$ as $w \to w_0$ but in a higher-order term.

To determine Λ we again need to match the inner limit of (3.12) with the outer limit of (A.5). To this end we expand $\bar{q}$ as $\eta \to \infty$ giving

$$\bar{q} = 2e^{-\eta} \int^{\eta^{1/2}} e^{w^2}\, dw = \sum_{n=0}^{\infty} \frac{(2n)!}{2^{2n} n! \eta^{n+1/2}}. \tag{A.6}$$

Writing the outer expansion (3.14) in terms of the inner variable η gives

$$\epsilon^n q_n \sim \frac{i\Lambda\epsilon^{1/2}\Gamma(n - 1/2)}{\eta^{n-1/2}} \qquad \text{as } n \to \infty. \tag{A.7}$$

Matching (A.6) and (A.7) gives

$$\Lambda = \frac{\beta e^{-5i\pi/4}}{2} \lim_{n\to\infty} \frac{(2n)!}{2^{2n} n! \Gamma(n + 1/2)} = \frac{\beta e^{-5i\pi/4}}{2\sqrt{\pi}}.$$

REFERENCES

[1] T.R. Akylas and T.-S. Yang, *On short-scale oscillatory tails of long-wave disturbances*, Stud. Appl. Math., 94 (1995), pp. 1–20.

[2] M.V. Berry, *Uniform asymptotic smoothing of Stokes's discontinuities*, Proc. Roy. Soc. London Ser. A, 422 (1989), pp. 7–21.

[3] J.G. Byatt-Smith, *On the existence of homoclinic and heteroclinic orbits for differential equations with a small parameter*, European J. Appl. Math., 2 (1991), pp. 133–158.

[4] S.J. Chapman, *On the rôle of Stokes lines in the selection of Saffman-Taylor fingers with small surface tension*, European J. Appl. Math., 10 (1999), pp. 513–534.

[5] S.J. Chapman, J.R. King, and K.L. Adams, *Exponential asymptotics and Stokes lines in nonlinear ordinary differential equations*, Proc. Roy. Soc. London Ser. A, 454 (1998), pp. 2733–2755.

[6] O. Costin, *On Borel summation and Stokes phenomena for rank-1 nonlinear systems of ordinary differential equations*, Duke Math. J., 93 (1998), pp. 289–344.

[7] G.D. Crapper, *An exact solution for progressive capillary waves of arbitrary amplitude*, J. Fluid Mech., 2 (1957), pp. 532–540.

[8] R. Combescot, V. Hakim, T. Dombre, Y. Pomeau, and A. Pumir, *Analytic theory of the Saffman-Taylor fingers*, Phys. Rev. A, 37 (1988), pp. 1270–1283.

[9] R.B. Dingle, *Asymptotic Expansions: Their Derivation and Interpretation*, Academic Press, London, 1973.

[10] R. Grimshaw and N. Joshi, *Weakly nonlocal solitary waves in a singularly perturbed Korteweg–de Vries equation*, SIAM J. Appl. Math., 55 (1995), pp. 124–135.

[11] V. Hakim, *Computation of transcendental effects in growth problems: Linear solvability conditions and nonlinear methods*, in Asymptotics Beyond All Orders, NATO Adv. Sci. Inst. Ser. B Phys. 284, H. Segur, S. Tanveer, and H. Levine, eds., Plenum, New York, 1991, pp. 15–28.

[12] A.C. King and M.I.G. Bloor, *A note on the free surface induced by a submerged source at infinite Froude number*, J. Austral. Math. Soc. Ser. B, 30 (1988), pp. 147–156.

[13] W. Kinnersley, *Exact large amplitude capillary waves on sheets of fluid*, J. Fluid Mech., 77 (1976), pp. 229–241.

[14] M.D. Kruskal and H. Segur, *Asymptotics beyond all orders in a model of crystal growth*, Stud. Appl. Math., 85 (1991), pp. 129–181.

[15] A.B. Olde Daalhuis, S.J. Chapman, J.R. King, J.R. Ockendon, and R.H. Tew, *Stokes phenomenon and matched asymptotic expansions*, SIAM J. Appl. Math., 55 (1995), pp. 1469–1483.

[16] E.O. Tuck and J.-M. Vanden-Broeck, *Ploughing flows*, European J. Appl. Math., 9 (1998), pp. 463–483.

[17] Y. Pomeau, A. Ramani, and B. Grammaticos, *Structural stability of the Korteweg-de Vries solitons under a singular perturbation*, Phys. D, 31 (1988), pp. 127–134.